LA-UR-73-1594

Conf-730836--3

TITLE: EXPERIMENTS WITH LASER-PRODUCED PLASMAS: ELECTRONS, IONS AND NEUTRONS

AUTHOR(S): R. P. Godwin

SUBMITTED TO: Presented at the Third Workshop on "Laser Interaction and Related Plasma Phenomena" held at Rensselaer Polytechnic Institute, Troy, New York, August 13-17, 1973.

By acceptance of this article for publication, the publisher recognizes the Government's (license) rights in any copyright and the Government and its authorized representatives have unrestricted right to reproduce in whole or in part said article under any copyright secured by the publisher.

The Los Alamos Scientific Laboratory requests that the publisher identify this article as work performed under the auspices of the U. S. Atomic Energy Commission.

los alamos
scientific laboratory
of the University of California
LOS ALAMOS, NEW MEXICO 87544

NOTICE

This report was prepared as an account of work sponsored by the United States Government. Neither the United States nor the United States Atomic Energy Commission, nor any of their employees, nor any of their contractors, subcontractors, or their employees, makes any warranty, express or implied, or assumes any legal liability or responsibility for the accuracy, completeness or usefulness of any information, apparatus, product or process disclosed, or represents that its use would not infringe privately owned rights.

DISTRIBUTION OF THIS DOCUMENT IS UNLIMITED

Form No. 836
St. No. 2629
1/73

UNITED STATES
ATOMIC ENERGY COMMISSION
CONTRACT W-7405-ENG. 36

EXPERIMENTS WITH LASER-PRODUCED PLASMAS: ELECTRONS, IONS, AND NEUTRONS [+] [*]

R. P. Godwin

Los Alamos Scientific Laboratory

University of California, Los Alamos, New Mexico 87544

ABSTRACT

Experimental results, particularly x-ray bremsstrahlung and ion time-of-flight measurements, obtained from plasmas generated with a 10 J, 25 psec Nd:YAG-Nd:glass (1.06 μm) laser delivering focal spot intensities of greater than 10^{16} W/cm^2 are reviewed. Preliminary experiments with a 10 J, 1 nsec CO_2 (10.6 μm) laser delivering $\sim 10^{14}$ W/cm^2 to a target are briefly discussed. Both sets of experiments yield high-energy (tens of keV) electrons and ions. Experimental evidence indicates that neutron emission can be explained by electron heating and a consequent ion acceleration. Therefore, neutron production in laser-produced plasmas can be a delusive diagnostic.

[+] A report of work performed under the auspices of the U. S. Atomic Energy Commission by G. H. McCall, A. W. Ehler, D. Giovanielli, R. P. Godwin, J. F. Kephart, K. B. Mitchell, T. F. Stratton, and F. Young.

[*] Presented at the Third Workshop on "Laser Interaction and Related Plasma Phenomena" held at Rensselaer Polytechnic Institute, Troy, New York, August 13-17, 1973.

INTRODUCTION

Very high target compressions (densities greater than one thousand times normal density) appear necessary if we are to obtain significant thermonuclear yields from laser-irradiated targets with lasers built using technology now available or expected soon.[1,2,3] While the hydrodynamics calculations of yield from laser-driven target implosions seems to be well understood, certain features of the problem are not. Major problem areas which require experimental and theoretical clarification include:

1. Laser absorption in plasmas

Which instabilities dominate the interaction of intense laser pulses with short lengths of plasma having steep density gradients? Do these instabilities lead to enhanced absorption or reflection?

2. Hot electrons

What is the number and energy distribution of nonthermal electrons created in laser-heated plasmas? How do these electrons influence target implosions?

3. Wavelength dependence

How are the absorption processes and the production of "hot" electrons influenced by laser wavelength? Must we use ultraviolet lasers to achieve laser-initiated fusion?

4. Compression

When significant target compression is achieved laser fusion will have been shown to be a viable concept.

You may notice that neutron generation has not been listed above. We do not consider neutron diagnostics a primary experimental diagnostic (at least until larger yields than have thus far been reported are achieved).

Numerous laser-plasma experiments have been performed at Los Alamos in the last year and a half. Most of our experiments have been attempts to understand the coupling of energy into a laser plasma. We have done, for example, experiments on backscattered and specularly scattered 1.06 μm radiation and upon the creation of doubled 1.06 μm, i.e., 0.53 μm light.[4,5] In concise summary, we have found in the interaction work that the light is absorbed in an extremely thin layer and that the plasma density profile is probably crucial in determining the interaction characteristics.

We shall concentrate in this discussion on electron-energy spectra and fast-ion emission. After relating these features to one another through an energy flux-limit condition, we will use them as the basis for a discussion of nonthermal neutron production in laser-produced plasmas.

A Nd:glass laser with a YAG oscillator has been used in most of our experiments. The pulse length is 25 psec as measured by

two-photon fluorescence. We have delivered more than 15 J to targets. We normally operate at less than about 12 J because the lack of isolation allows backscattered light to damage the laser. The focal diameter is less than 50 μm giving us a power at focus of greater than 10^{16} W/cm^2. While the 10 to 15 J laser energy is not large, we have laser powers comparable with any being used because of the short pulse length. Figure 1 is a schematic of the small laser which is like the preliminary stages of the larger glass system (> 1 kJ) being constructed at Los Alamos. The mode-locked dye oscillator is followed by a Pockel's cell switch to select a single pulse from the Q switched train of pulses and then by two 10 mm YAG amplifiers followed by a 20 mm and finally a 51 mm glass amplifier. Note the divergence of the beam through the glass amplifiers. This divergence appears to alleviate self-focusing problems in the 51 mm rod.

An aspheric f/3.5 focusing lens with a 70 mm focal length delivers our beam to targets. Most of our experiments have been performed with thin films of CH_2 as targets; although we have also used deuterated polyethylene as well as various metal films, small carbon spheres, and metal wires.

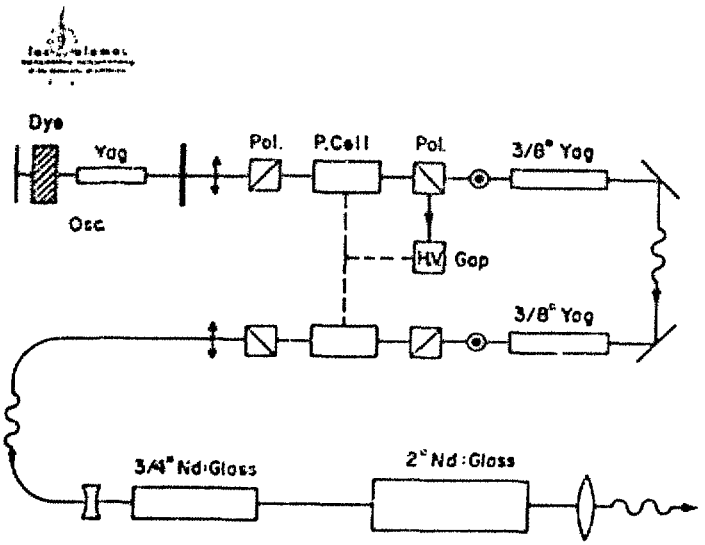

Fig. 1. Schematic diagram of the Los Alamos 10 J, 25 psec Nd:YAG--Nd:glass laser system.

ELECTRONS

At the time of the last RPI Workshop it was becoming evident that high-energy electrons were created in laser-produced plasmas.[6] The only information available was that the electrons had a very nonthermal character and that high-energy electrons were present. We believe that a small number of electrons, perhaps 10^{10}, may escape the plasma completely until an electrostatic barrier is set up to prevent further electron escape. While we have attempted to directly measure escaping electrons, we have not succeeded in doing so. Perhaps the most direct evidence of escaping electrons is the x-ray measurements performed at Garching in which x rays have been shown to be created at the walls of the target chamber.[7] Figure 2 shows what may be indirect evidence of escaping electrons. Magnetic fields[8] were being measured with a small loop probe near the laser plasma. In the figure one sees the signature of a magnetic field as the characteristic negative-positive pulse. This signal, as expected, inverts if one turns the probe 180°. The other signal early in time does not invert. We believe this early signal may be due to electrons escaping from the plasma leaving it positively charged.

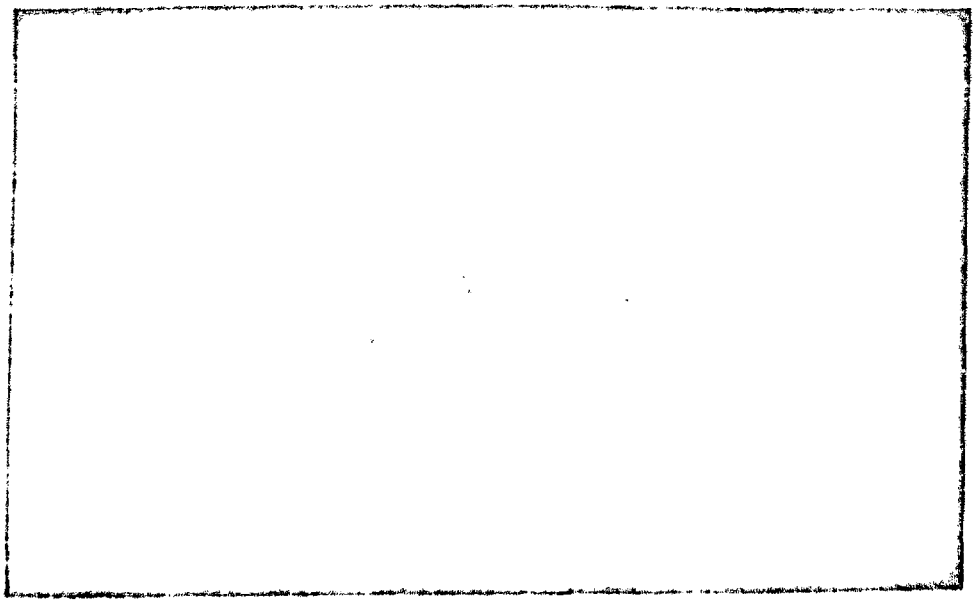

Fig. 2. Raw data obtained with a magnetic probe 1.5 cm from a laser-produced plasma in high vacuum. The negative-positive pulse represents a magnetic field at the probe of a few gauss. The early fast signal may be due to electrons escaping from the plasma.

In effect, the signal is that of an instantaneously charged capacitor. If one knew the geometry of the plasma one would be able to determine from the signal the number of electrons leaving the plasma. While we are not able to do that accurately, the signal is consistent with the interpretation above.

We turn briefly to an experiment which has been discussed quite a lot in the past year and perhaps overemphasized. We have constructed a classical x-ray polarimeter.[9,10] The polarimeter consists of a thin plastic scatterer with four detectors as nearly identical as possible located on the symmetrical spokes of a detector assembly. The detectors are NaI(Tl) scintillators coupled to conventional photomultiplier tubes. Since Compton scattering is polarization dependent, one can measure the polarization by determining the asymmetry in signals of the various detectors. Conceptually, this is a very simple experiment; practically it is quite difficult. One would like to learn from such a measurement the electron velocity distribution in the plasma as a function of angle. The interpretation of polarization measurements depends on whether the electrons are creating bremsstrahlung in what is essentially a thick or thin target, i.e., whether or not the electrons make multiple scatterings in their transit of the radiating volume. The photon-energy acceptance in the detectors relative to the maximum electron energies radiating the x-ray spectrum is particularly important. Backgrounds, experimental asymmetries, solid-angle depolarization, and multiple scattering in the scatterer must all be considered. The influence of background radiation is difficult to eliminate. Since the scatterer has an efficiency $\sim 10^{-4}$, a small number of hard-to-shield 100 keV or higher energy x rays can falsify measurements. Since we have not been able to sort all of these factors to our satisfaction, we have not formally published the results of this experiment. We do, however, believe that we have measured a polarization of the order of 15% in the laser-plasma x rays. The polarization appears to be such that electrons are moving preferentially along the k vector of the incident laser beam, i.e., not parallel to the electric vector of the incident radiation. The Garching group has attempted to find an asymmetry in x-ray emission from laser plasmas. Within the errors of their experiment, they found no asymmetry.[7] Whether or not there can be a marked asymmetry of electron excitation in laser plasmas is, in our opinion, still an open question.

Most experiments measuring x-ray spectra in laser plasmas have used filter techniques for channel energy selection. This is an easy method to implement, but is a difficult one to interpret. We have constructed a multiple-channel x-ray spectrometer[11] which is more difficult to operate than filtered detectors, but for which data are essentially trivial to interpret. The spectrometer consists of a number of flat Bragg crystals with detectors located at

the proper angles to accept energy diffracted from the various crystals. The detectors are NaI(Tl) scintillator-photomultiplier combinations. While the spectrometer has the capability of eight detector channels, it is at present operating with six channels at energies of 4.3, 6.9, 11.2, 18.5, 30.3, and 50.4 keV. The resolution $\Delta E/E$ is typically $\sim$ 20%. All the channels, except that at the highest energy, have pyrolytic graphite diffraction crystals. The highest energy channel uses a 200 plane in lithium fluoride. In Fig. 3 are exhibited four x-ray spectra randomly chosen from a large number of measurements. No two measurements are identical, although all have certain similarities. The channel at 50 keV has the smallest signals and is also near the direct beam of x-rays through the spectrometer so that statistical fluctuations and background signals are most likely to influence it. The 4.3 and 6.9 keV channels are less accurately calibrated than are the higher energy channels. The most dependable channels are those in the 10 to 30 keV region. Note that in a single instrument measurements are obtained over four decades in intensity. The spectrometer channels are calibrated (with a conventional x-ray tube) relative to one another quite well and absolutely to about a factor of two. Although nonthermal

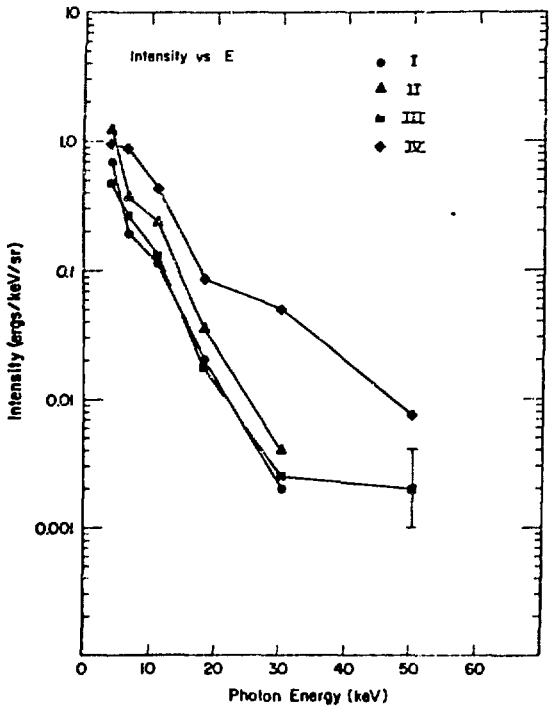

Fig. 3. X-ray spectra obtained with a multiple crystal spectrometer viewing a CH_2 target irradiated by nominally 1.0 J, 25 psec 1.06 μm laser pulses. The absolute intensity assumes isotropic radiation.

electrons exist in these experiments, a semi-log plot of x-ray intensity vs photon energy is fairly linear. This implies that we can define a "temperature" $k_b T$. The slope of the curves yields an effective hot-electron temperature of about 10 keV. We should point out that the spectra also fit reasonably well a dependence $\sim \exp(v/v_o)$, where v is the electron velocity. The tail of the electron distribution suggested by Kruer would give such a spectrum.[12]

IONS

Ion emission from our laser-produced plasmas has been examined with several techniques.[13] Ion collectors constructed using commercial BNC feedthroughs with grids provided for applying various voltages to check spurious effects have been the primary diagnostic. Figure 4 shows a spectrum obtained with such ion detectors viewing a laser irradiated CH_2 foil target. It is a direct tracing of an oscilloscope record. Initially, one sees a large spike which is a photoelectron signal due to the x-rays and extreme ultraviolet radiation emitted by the plasma. Then we find a string of jagged peaks. We identify the first of these as protons and those following as

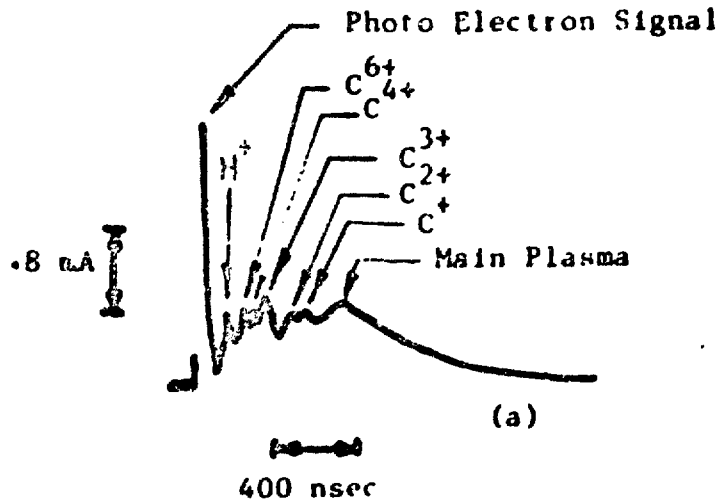

Fig. 4. Ion collector current as a function of time for laser-plasma experiments with a CH_2 target.

carbon in various ionization states. The final broad peak is due to a cool neutral plasma. On the side opposite a thin (25 μm) target from the laser, one sees a cold plasma, but none of the ion spikes. We interpret the ion-current spikes as being due to essentially electrostatically-accelerated ions associated with hot electron production. A consistent fit is obtained if one identifies the spikes with the energy being Z (the ionic charge state) times a constant voltage. The ion-collector information alone may not be convincing; but we have another detector, the Thomson parabola, which allows the unambiguous determination of the charge-to-mass ratio of plasma ions. We use a design developed by Kuswa at Sandia Laboratories. Figure 5 is a photographic record obtained with the device. The bright point in the lower-right-hand corner of the photo is a pinhole image of the laser-produced plasma. The parabolas (from left to right) are protons and three charge states in carbon. (In raw data one can often see more than three charge states.) The vertical displacement from the pinhole picture of the plasma to the start of the parabolas gives the maximum energy of ions present. For instance, the proton trace of Fig. 5 contains energies up to 50 keV. Thomson parabola records are consistent with the interpretation of the ion collector data discussed above.

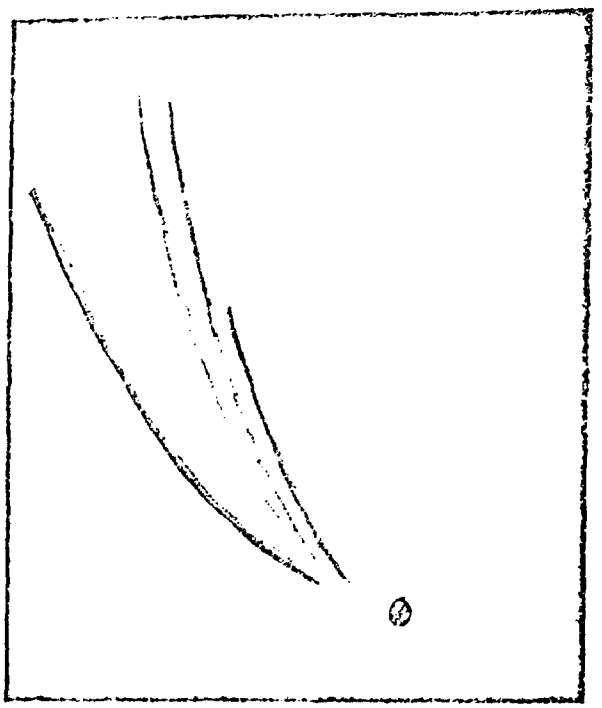

Fig. 5. Thomson parabola record obtained with laser-produced plasma from a CH_2 target. The bright spot in the lower-right-hand corner is an image of the plasma. The parabolas (from left to right) are protons and various charge states of carbon.

CO_2 LASER EXPERIMENTS

We have recently begun experiments with the short pulse CO_2 laser being developed at Los Alamos by the group of Dr. Fenstermacher. The laser has been discussed at this Workshop.[14] The laser wavelength is 10.6 μm. The pulse length is about 1.5 nsec FWHM. It has a very fast rise time and a much slower decay, as one would expect from saturated amplifiers. As yet we are not sure how much energy is in the wings of the pulse. We have delivered up to about 15 J to a target. We believe the focal diameter is about 80 μm, giving us a power upon targets $\sim 10^{14}$ W/cm^2--the highest yet achieved in 10.6 μm laser-produced plasmas. The laser-plasma diagnostics we have thus far performed are indicated schematically in Fig. 6. We are using the first three amplifier stages of the laser. The beam is deflected 90° by a turning mirror. A hole in that mirror allows a photon-drag detector to view a portion of the beam to study its time dependence. The beam is brought to focus on targets which, to this time, have been CH_2 films by an f/3.5 silver coated off-axis parabolic aluminum mirror with a 10 cm focal length.

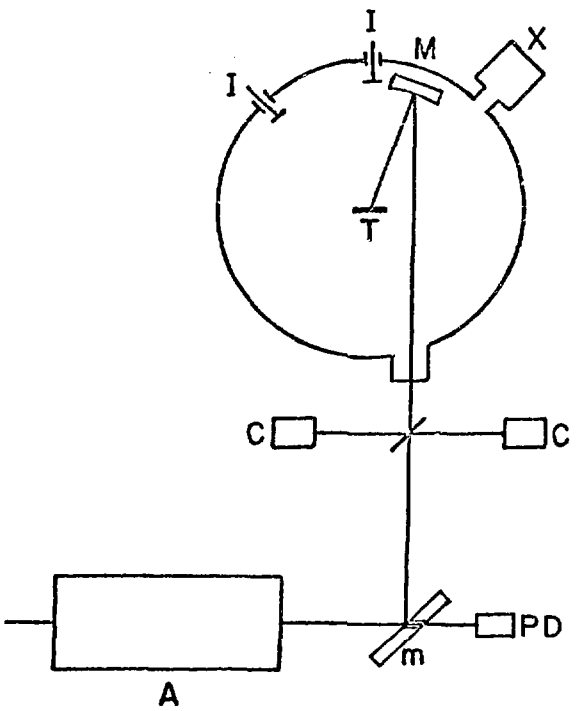

Fig. 6. Schematic diagram of the initial diagnostics of target interaction experiments with the Los Alamos 1.5 nsec CO_2 laser.

We have a NaCl pellicle for reflection of a known fraction of the beam into calorimeters for measuring the incident and backscattered radiation intensities. A number of filter type x-ray detectors and ion current collectors view the target. In these preliminary experiments we have measured backscattered fractions of 2 to 6% with a lot of scatter, perhaps due to focusing difficulties. Table I is a summary of three shots chosen from our preliminary CO_2 measurements.

TABLE I

Energy Inc. (J)	Backscatter (%)	X-Ray "Temp." (keV)	X-Ray Energy $\gtrsim$ 8 keV (erg/sr)
9.8	3.6	$\sim$ 10	45
5.4	2.8	$\sim$ 15	10
7.5	2.1	$\sim$ 10	12

The x-ray "temperature" was defined by using filtered detectors with three channels in the region of about 8 to 40 keV. The temperatures from different detector combinations are not identical. In Fig. 7 we have exhibited ion current as a function of energy per

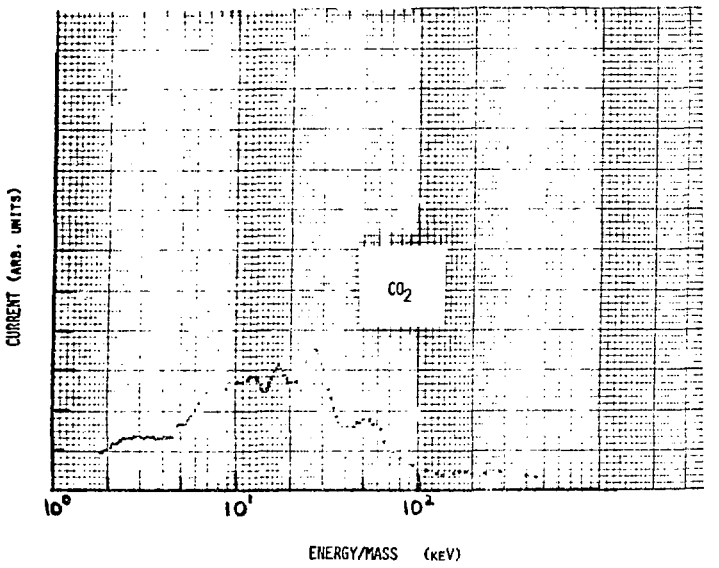

Fig. 7. Ion collector current as a function of energy per unit atomic mass for a CH_2 plasma created with a $\sim$ 10 J, 1.5 nsec CO_2 laser pulse. Note the 50 keV proton peak.

unit atomic mass for a laser plasma created by irradiating CH_2. We identify the peak at 50 keV as protons and the other peaks as various ionization states in carbon.

In summary, plasmas produced by 10 J pulses from both a 1 nsec CO_2 laser and a 25 psec Nd:glass laser contain high-energy electrons with an effective average energy of about 10 keV as determined by x-ray measurements and ions with energies of 50 keV or greater.

FLUX LIMIT FOR ELECTRON HEATING

Consider the implications for x-ray and ion measurements of the flux-limit condition of Morse and Nielson which was briefly discussed at this workshop by Morse.[15] First let us review some x-ray physics. The integrated bremsstrahlung radiation emitted by an electron in a thick target x-ray tube with an anode of atomic number Z is well approximated by[16,17]

$$I_x = kZ\ E^2, \tag{1}$$

where $k \simeq 0.7 \times 10^{-6}$ when the intensity I_x and the electron energy E are both in keV. We wish to estimate the x-ray emission from our laser plasmas. We assume that a small region at the surface of the target (at or near the critical density where the electron plasma frequency equals the laser frequency) is heated and that electrons leave that region and emit x-rays in a denser cold region behind the laser-electron interaction region--an emission model similar to conventional thick target x-ray emission. The bremsstrahlung emission can be estimated as

$$I_x = N_h\ k\ Z \langle E_x^2 \rangle, \tag{2}$$

where N_h is the number of hot electrons and $\langle E_x^2 \rangle$ is an appropriate electron energy squared averaged over the electron distribution function present in the plasma. Detailed calculations support the validity of this simple picture.[18]

The flux-limit condition of Morse and Nielson requires that the absorbed laser power is equal to the energy flux carried away from the interaction region by hot electrons, i.e.,

$$P_L = \tfrac{1}{2} \int mv^2\ v\ f(v)\ dv; \tag{3}$$

where P_L is the laser power, m and v are respectively the electron mass and velocity, and f(v) is the electron distribution function. We represent the integral by

$$P_L = \tfrac{1}{2}\ m\ n_h \langle v^3 \rangle, \tag{4}$$

where n_h is the hot electron density and $\langle v^3 \rangle$ is an average over the distribution function. This representation of the flux limit can be used to estimate N_h and $\langle E_x^2 \rangle$; and thus the x-ray emission. We define an average energy $\langle E \rangle$ or "temperature" k_bT as

$$\langle E \rangle \equiv \tfrac{1}{2} m \langle v^2 \rangle \simeq \tfrac{1}{2} m \langle v^3 \rangle^{2/3} . \qquad (5)$$

Now let us assume that the number density of hot electrons n_h is equal to the critical density n_c. Then using the flux limit condition we find that the effective electron energy is

$$\langle E \rangle \simeq \left(\tfrac{1}{2} m\right)^{1/3} \left(P_L/n_c\right)^{2/3} . \qquad (6)$$

Notice that the average energy contains the ratio of the laser power to the critical density. This ratio can be considered a "reduced intensity". In our 1.06 μm experiments we have a critical density of 10^{21} electrons/cm^3 with a laser power of about 10^{16} W/cm^2, while in our 10.6 μm experiments we have n_c equal 10^{19} and P_L equal 10^{14}. Both of our experiments have approximately the same "reduced intensity" and according to the flux limit, both should give effective electron energies or temperatures of $\sim$ 10 keV. This prediction is in qualitative agreement with the x-ray spectral measurements discussed earlier. The $\langle E \rangle$ given by Eq. (6) is not the proper energy for calculation of x-ray intensity according to Eq. (2). We require the average square of the electron energy. Since x-ray spectral measurements do not uniquely determine electron spectra, we cannot directly measure the electron distribution function with x-ray spectroscopy. However, since the x-ray measurements performed with the Bragg spectrometer are consistent with a Maxwellian energy distribution we will assume such a distribution is present. One thus finds

$$\langle E_x^2 \rangle = \int E^2 f(E)\, dE \,/ \int f(E)\, dE = 3.75 \langle E \rangle^2 . \qquad (7)$$

The simplest estimate of N_h, the number of hot electrons, is obtained by assuming all the laser energy E_L is initially deposited in electrons at the average energy $\langle E \rangle$. In that case

$$N_h \simeq E_L \,/\, \langle E \rangle ; \qquad (8)$$

with the laser energy 10 J and the electron temperature 10 keV we find $N_h \sim 6 \times 10^{15}$ electrons. An alternate estimate of N_h can be obtained by assuming N_h is equal to the critical density times the volume of the interaction region multiplied by a "turnover factor." The turnover factor is necessary since, during the laser pulse, electrons are heated and leave the interaction volume to be replaced by cold electrons which are in turn heated and leave the volume. The turnover factor can be approximated by the laser pulse length divided by the time required for an electron to leave the interaction

volume (roughly the interaction region thickness divided by an average electron velocity which can be estimated using the flux-limit condition). Thus

$$N_h \simeq n_c \, A \, t \, \tau_L \div (t \, / \langle v \rangle) = n_c \, A \, \tau_L \langle v \rangle , \qquad (9)$$

where A is the focal area, t the interaction region thickness, τ_L the laser pulse length, and $\langle v \rangle$ the average hot-electron velocity. In this picture N_h is independent of the interaction thickness. We have, using the flux-limit condition,

$$N_h \simeq (n_c \, A \, \tau_L)^{2/3} \quad (2 \, E_L \, / \, m)^{1/3} . \qquad (10)$$

The quantity $n_c \tau_L$ is roughly the same in both our 1 and 10 μm experiments. For our Nd laser experiments N_h estimated by Eq. (10) is $\sim 4 \times 10^{15}$ electrons.

Upon inserting estimates $N_h \sim 5 \times 10^{15}$ and $\langle E_x^2 \rangle \sim 375$ into Eq. (2), we find that with 10 J incident on a CH_2 ($Z \simeq 6$) target we expect $\sim 10^{13}$ keV or $\sim 10^4$ ergs to be emitted as bremsstrahlung x rays. This is an x-ray production efficiency, $e_x \equiv I_x \, / \, E_L$, of $\sim 10^{-4}$, in qualitative agreement with our measurements of the x-ray emission intensity and with those of other laboratories.[19] It appears that, qualitatively at least, the flux-limit condition with essentially all the laser energy assumed to initially reside in hot electrons is consistent with both the effective "temperature" and absolute bremsstrahlung intensity obtained from our x-ray measurements performed with plasmas created by single short laser pulses.

The hot electrons implied by the flux limit condition lead to the creation of hot ions with energies of a few times the hot electron energy. The number of hot ions expected is a significant fraction of the hot-electron number. We measure $\sim 10^{15}$ ions with energies > 50 keV in both our Nd:glass and CO_2 experiments in rough agreement with the implications of the flux limit. We hope that with improvements in the theory of hot-ion production from electrons and in ion measurements that more useful comparisons can be made.

NEUTRONS

Let us briefly review the evidence for neutron production from laser-produced plasmas that was available several years ago.[20,21,22,23] With 1.06 μm Nd:glass laser pulses of a few nsec duration and a few joules or more of energy an enhanced reflectance and production of x rays and ions seemed correlated with the emission of small numbers ($\gtrsim 10^3$) neutrons from laser-produced plasmas. While there had been a small number of experiments performed with 10 μsec

pulses, no neutrons had been observed with the very short laser pulses, although apparently the x-rays, etc. associated with neutrons from longer pulses were observed. Hydrodynamics calculations have failed to give a convincing overall agreement with experimental neutron yields.

We performed some short-pulse experiments looking for neutrons at Los Alamos.[24] The experimental configuration is shown schematically in Fig. 8. We focused about 15 J onto a deuterated polyethylene film. We observed fast ions and x-ray production, but no neutrons. (Incidentally, we shielded our neutron detector with 3 cm of lead to remove hard x-ray signals from the neutron detector, while using a CH_2 target, before inserting CD_2.) After a few shots we began to measure a small number of neutrons. We carefully made a time-of-flight measurement by allowing a portion of the x-ray pulse to enter the neutron detector and then measuring the neutron arrival time relative to the x-ray signal. The time-of-flight measurements indicated that the neutrons were coming from the wall of the chamber--presumably from CD_2 deposited there. We then inserted CD_2 foils in front of and behind the CD_2 laser target. We found in

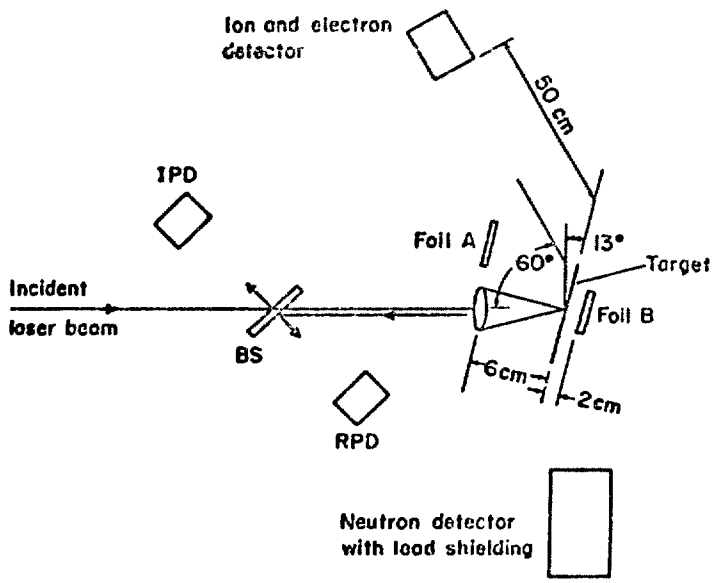

Fig. 8. Experimental layout for investigation of neutron generation with our 10 J, 25 psec Nd:glass laser. With this setup neutrons are generated at the secondary CD_2 target on the laser side of the primary CD_2 target.

this case an enhanced neutron emission as one would expect if deuterium ions formed at the CD_2 laser target interacted with deuterons in the foil in front of (i.e., on the laser side of) the laser target to produce neutrons. The presence of fast ions of an appropriate energy to explain the neutron time-of-flight measurements was confirmed by coincident measurements with an ion-current detector. Very few neutrons were emitted from the laser target itself or from the foil which was behind the target. The main features of this experiment have been reproduced by the Naval Research Laboratory.[25] We are convinced that our neutrons were not thermonuclear in origin, but were associated with fast-ion production.

The short-pulse experiments discussed above are not convincing evidence that the neutrons measured by other experimenters with longer pulse (few nsec) lasers were emitted by the same or a similar mechanism, but we became suspicious--especially since hydrodynamic code calculations of neutron emission are in poor or at least strained agreement with experiment. McCall pursued the idea of hot ions being associated with neutron emission and found a qualitatively, satisfactory explanation of several neutron production experiments for which he has been able to obtain sufficient information for comparison with his theory.[26] Several other theories of nonthermal neutron production have been proposed.[27]

We digress to remind you of the Gamow tunneling factor for D-D reactions. The D-D cross section is[28]

$$\sigma_{DD} = \frac{288}{E_i} \exp(-45.8/E_i^{\frac{1}{2}}), \qquad (11)$$

where σ_{DD} is in barns and the deuteron energy E_i is in keV. The ion energy in the exponential is by far the dominant factor in determining the cross section. For example, using Eq. (11), the ratio of cross sections for 30 keV deuterons to that for 3 keV deuterons is greater than 10^6. It is obvious that a small number of high-energy deuterons can make a very significant contribution to neutron production.

Consider the production of neutrons by plasmas produced with nsec pulse length lasers keeping in mind the possible importance of high-energy ions. If a laser pulse is incident on a cold plasma with a steep density profile, a plasma is created of blown off material in front of the surface. Instabilities may then create hot electrons and consequently hot ions near the critical density. These hot ions stream out through the cold blowoff material. With this situation we have in effect a cold secondary ion-target material, which in the case of our shorter pulse experiment was replaced by a foil of CD_2 in front of the laser target. That the neutrons from a nsec pulse laser experiment do indeed come from the target region, as this model suggests, has been verified by Yamanaka.[29]

We expect a neutron generation rate

$$R_n = n_i v_i N_b \sigma (E_i), \tag{12}$$

where $n_i v_i$ is the hot-ion flux and N_b is the number of blowoff ions that the hot ions stream through. The neutron generation rate is independent of the distribution of plasma in front of the critical density. It depends only on the integral N_b of that distribution, which can be estimated from scaling laws. The argument of the exponential in σ_{DD} dominates Eq. (12), so we will discuss only that term here (although in the more complete formulation of these ideas[26] all the factors are considered to give not only the energy dependence of neutron production but also an absolute numerical prediction).

We return to the flux-limit condition[15] and let

$$P_L = \alpha \tfrac{1}{2} m n_h v_h^3; \tag{13}$$

a slightly different formulation of the flux limit than that we used earlier. The α has been introduced as a phenomenological parameter and v_h is an effective hot-electron velocity. McCall has introduced another factor β, where $n_h = \beta n_c$; β is essentially the fraction of hot electrons effective in producing hot ions. In this formulation

$$v_h = (2 P_L / m n_c \alpha\beta)^{1/3}. \tag{14}$$

One further finds that the energy of the hot ions produced by the electrostatic sheath due to hot electrons is proportional to v_h^2. This relation between hot electrons and hot ions gives us the dominant factor in the energy dependence of the neutron production through the exponential of the Gamow tunneling factor. The important parameter $\alpha\beta$ can be determined experimentally from the ion energy E_i measured in an experiment for calculation of neutron production in that experiment. McCall finds the neutron production/ cm^2 is given by

$$N = A \alpha^{1/3} \beta^{7/3} \lambda^{-14/3} P_L^{-1/3} \exp\left\{ -B(\alpha\beta)^{1/3} \lambda^{-2/3} P_L^{-1/3} \right\}, \tag{15}$$

where λ is the laser wavelength and A and B are constants.

We summarize McCall's numerical results with graphs. In Fig. 9 we have plotted measured ion energy in keV vs incident laser intensity in W/cm^2 for Nd:glass lasers. The points are ion-energy measurements which were presented by Yamanaka at the 1971 RPI Workshop.[22] The $\alpha\beta$ determined phenomenologically in this way is

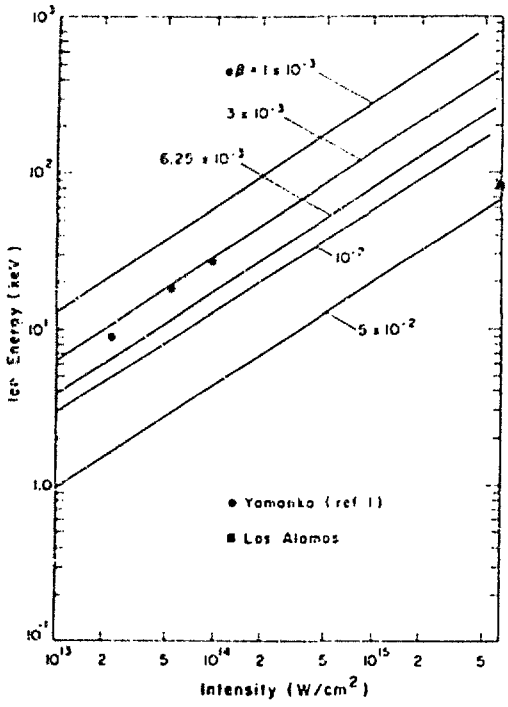

Fig. 9. Fast-ion energy as a function of laser energy for various values of the parameter $\alpha\beta$ which relates fast ions to hot electrons. Data from the work of Yamanaka and McCall are indicated.

about 3×10^{-3} in those experiments. For our 25 psec experiments we find the larger $\alpha\beta \simeq 5 \times 10^{-2}$. (We note parenthetically that these $\alpha\beta$ values appear reasonable on theoretical grounds, but we are using experiments to determine $\alpha\beta$.) Figure 10 is measured neutron number vs laser energy for the experiments of Yamanaka (triangles) and Floux (circles) discussed at the last Workshop.[21,22]

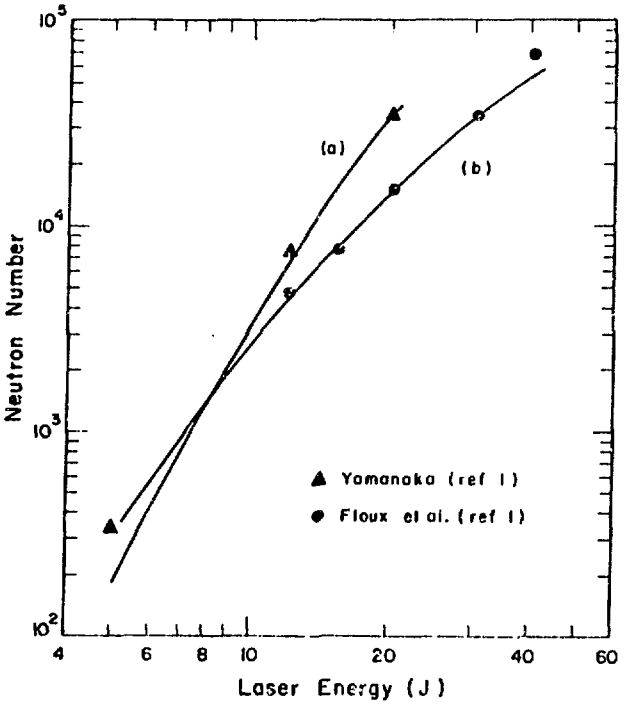

Fig. 10. Neutron yield as a function of laser energy for experiments of Yamanaka and Floux and a fit to these data using McCall's fast-ion neutron generation mechanism.

The solid lines are predictions of the model under discussion. For Yamanaka's experiment a slight fitting, by varying individually α and β, has been used to fit the absolute neutron number; while the scaling with energy is dependent only upon the $\alpha\beta$ fixed by Yamanaka's ion measurements. Since no ion measurements were reported by Floux, McCall has assumed an $\alpha\beta$ to obtain the displayed fit to Floux's experiment. This model in which hot electrons lead to accelerated ions and thus neutrons may be meaningful in the interpretation of many low-energy laser-neutron experiments.

An interesting feature of this neutron generation model is that the generation rate is given explicitly as a function of laser wavelength. Figure 11 is predicted neutron generation as a function of wavelength for various laser intensities. For Nd:glass and CO_2 irradiation at 10^{14} W/cm^2 (roughly 10 J in 1 nsec) one expects about an order of magnitude fewer neutrons from CO_2 than glass. We believe that the hydrodynamics codes, which have been fitted to 1.06 μm laser-produced neutron experiments predict much lower neutron yields than this for 10.6 μm CO_2 laser experiments. We hope soon to make measurements at Los Alamos which will check this aspect of the theory.

Even if laser-produced neutrons reported to date have not been created in the manner described above, the model points out that neutrons can be a delusive diagnostic in laser-plasma experiments aimed at fusion. We believe that experiments which give conclusive evidence of the attainment of high compressions in laser targets are particularly important.

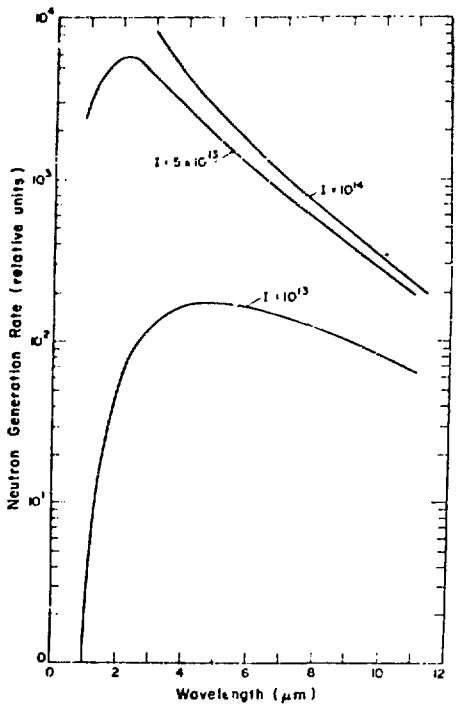

Fig. 11. Predicted neutron generation rate as a function of laser wavelength for $\alpha\beta = 3 \times 10^{-3}$.

REFERENCES

1. This Workshop published as:
Laser Interaction and Related Plasma Phenomena Vol. III (H. Schwarz and H. Hora, eds.) Plenum Press, New York. See contributions by K. A. Brueckner, R. E. Kidder, R. L. Morse, and J. Nuckolls.

2. K. Boyer, Astronaut. Aeronaut. 11, 28 (1973).

3. J. Nuckolls, J. Emmett, and L. Wood, Phys. Today (August 1973) p. 46.

4. G. H. McCall, R. P. Godwin, and J. F. Kephart, Bull. Am. Phys. Soc. 17, 1044 (1972) and unpublished work.

5. Our work agrees in most aspects with that of other researchers. See, for example, Laser Interaction and Related Plasma Phenomena Vol. III, contributions by J. L. Bobin and R. Sigel.

6. See, for example:
K. Büchl, et al., Laser Interaction and Related Plasma Phenomena Vol. II, p. 503 and J. W. Shearer et al., Phys. Rev. A6, 764 (1972).

7. K. Eidmann and R. Sigel, VI European Conf. on Controlled Fusion and Plasma Physics, Moscow, July 30-August 3, 1973, and R. Sigel, this Workshop.

8. D. Giovanielli, Los Alamos Scientific Laboratory (Internal report). For discussions of magnetic fields associated with laser plasmas see Laser Interaction and Related Plasma Phenomena Vol. III contributions by F. Schwirtzke and J. A. Stamper.

9. R. P. Godwin, J. F. Kephart, and G. H. McCall, Bull. Am. Phys. Soc. 17, 971 (1972).

10. A. H. Compton and S. K. Allison, X Rays in Theory and Experiment, 2nd ed. (Van Nostrand, New York, 1935), p. 93.

11. J. F. Kephart, R. P. Godwin, and G. H. McCall, Bull. Am. Phys. Soc. 17, 971 (1972).

12. W. Kruer in Laser Interaction and Related Plasma Phenomena Vol. III.

13. A. W. Ehler, D. Giovanielli, and F. Young, Anomalous Absorption Conf., Los Alamos, March 1-2, 1973.

14. R. S. Cooper in Laser Interaction and Related Plasma Phenomena Vol. III.

15. R. L. Morse and C. W. Nielson, Phys. Fluids, 16, 909 (1973) and R. L. Morse, this Workshop.

16. A. H. Compton and S. K. Allison, X Rays in Theory and Experiment, 2nd ed. (Van Nostrand, New York, 1935) p. 104.

17. R. D. Evans, The Atomic Nucleus (McGraw-Hill, New York, 1955) p. 614.

18. W. P. Gula, Los Alamos Scientific Laboratory (private communication).

19. See, for example: C. E. Violet, et al., IEEE/OSA Conf. on Laser Engineering and Applications, Washington, D. C., May 30-June 1, 1973.

20. N. G. Basov, et al., Laser Interaction and Related Plasma Phenomena Vol. II, p. 389.

21. F. Floux, et al., Laser Interaction and Related Plasma Phenomena Vol. II, p. 409.

22. C. Yamanaka, Laser Interaction and Related Plasma Phenomena Vol. II, p. 481.

23. K. Büchl, et al., Laser Interaction and Related Plasma Phenomena Vol. II, p. 503.

24. G. H. McCall, et al., Phys. Rev. Letters 30, 1116 (1973).

25. J. A. Stamper in Laser Interaction and Related Plasma Phenomena Vol. III.

26. G. H. McCall, Los Alamos Scientific Laboratory, Report LA-UR-73-791 (to be published).

27. A. Caruso, Frascati (preprint) and J. Katz, Lawrence Livermore Laboratory (preprint).

28. S. Glasstone and R. H. Lovberg, Controlled Thermonuclear Reactions, (Van Nostrand, Princeton, 1960), p. 20.

29. C. Yamanaka in Laser Interaction and Related Plasma Phenomena Vol. III.